Lithuanian Journal of Physics
Vol. **65**, No. 3, pp. 162–172 (2025)

ISSN 1648-8504 eISSN 2424-3647
DOI: https://doi.org/10.3952/physics.2025.65.3.5

MECHANICAL STRESS, OPTICAL AND SURFACE PROPERTIES OF HIGH TEMPERATURE ANNEALED HfO_2, Sc_2O_3 AND Al_2O_3 BINARY MIXTURE THIN FILMS DEPOSITED BY ION BEAM SPUTTERING

G. Abromavičius

Optical Coating Laboratory, Center for Physical Sciences and Technology, Savanorių 231, 02300 Vilnius, Lithuania
Email: giedrius.abromavicius@ftmc.lt

Received 21 October 2025; revised 15 November 2025; accepted 20 November 2025

High compressive stress is one of the main drawbacks of ion beam sputtered coatings by deteriorating the flatness of optical components. Mixtures of high refractive index metal oxides with SiO_2 allow one to increase the laser induced damage threshold of multilayer stacks. Study of optical, surface roughness and stress properties of HfO_2–Al_2O_3, Sc_2O_3–Al_2O_3, HfO_2–Sc_2O_3 binary mixtures using a broad range of post-deposition thermal annealing up to 900°C is presented. Admixing Al_2O_3 in moderate concentrations to HfO_2 and Sc_2O_3 allows one to sustain a low surface roughness, to decrease the extinction of layers during thermal treatment, while obtaining –360…–560 MPa tensile stress after annealing to 500°C, depending on the particular mixture. The obtained data allow one to point out possible candidates – HfO_2(56%)–Al_2O_3(44%), Sc_2O_3(70%)–Al_2O_3(30%), HfO_2(~70%)–Sc_2O_3(~30%) – and the 500–600°C annealing temperature range for the design of stress compensated multilayer coatings for the UV spectral range with potentially increased laser induced damage threshold.

Keywords: ion beam sputtering, coating stress, material mixtures, UV range

1. Introduction

Ion beam sputtering (IBS) allows the deposition of complex multilayer optical coatings with low optical losses, precise and environmentally stable spectral characteristics. This technology is often preferred for manufacturing of optical components for the state-of-the-art laser systems, complex instruments like gravitational wave detectors, cavity ring-down spectrometers, etc. [1–3]. High compressive stress is a well-known drawback of IBS coatings [4–7] leading to the degradation of surface flatness [8], aberrations, and laser pulse wavefront distortion [9]. Thermal post-deposition treatment at optimized temperatures is one of the most effective technique to solve this problem. It might reduce stress close to zero value [8, 10–12], but it is not applicable to all or particularly temperature-sensitive substrates. Also it might induce crystallization of some coating materials and, respectively, increased roughness and optical scatter loss [13–15]. Recently, Steinecke et al. also demonstrated the reduction of IBS thick film stress using *in situ* heating [16]. The deposition of the backside coating (usually SiO_2 layer) of calculated thickness also might compensate for the stress of front side coating. Added manufacturing costs by the extra coating process are the main shortcoming in this case. *Ex situ* stress reducing methods are not suitable for very thin (sub-milimetre thickness) substrates, since high stresses can break down the substrates during the coating process. Therefore, *in situ* techniques were also investigated. The adjustment of assisting beam parameters in the dual ion beam sputtering (DIBS) process results in smaller stress within a growing film [17]. For example, the argon and oxygen ion (550 eV) mixture assistance resulted in stress decrease from ~230 to ~120 MPa [18].

Other studies revealed a considerable change of film stress, if using different process parameter values, such as partial oxygen pressure, the voltage of a primary ion source or substrate temperature [19, 20]. Using material mixtures also allows one to tune the stress of IBS optical coatings [21, 22], which could also be successfully combined with the thermal annealing procedure [8, 23]. The application of material mixtures also gives the tuning possibility of other important film properties like the refractive index, optical losses, band gap and laser damage performance [14, 24–30].

The choice of materials for IBS coatings for the ultraviolet (UV) spectral range is limited to mainly oxide materials HfO_2, Sc_2O_3 and Al_2O_3 as high refractive index (*H*) materials and SiO_2 as a low refractive index (*L*) material. Sputtered layers of these oxides also have high compressive stresses. For example, SiO_2 has ~550 MPa compressive stress which could be reduced after annealing [8]. HfO_2 films possess even higher 750 MPa compressive stress which also decreases after annealing [10]. Annealing of hafnia to high (>850°C) temperatures resulted in the change from compressive to tensile (≤400 MPa) stress [31]. Sc_2O_3 films also possess the initial compressive stress of 550–1300 MPa, depending on the process parameters [19]. Alumina films have compressive stresses of 390 MPa [32].

The thin film treatment using high temperatures for stress reduction could trigger its crystallization, which might induce scatter losses [15]. This is even more crucial for shorter wavelengths at the UV range. Several studies revealed the transition of hafnia films from the amorphous to polycrystalline phase after annealing to 500°C [10, 33–35] or using a considerably longer treatment time at 475°C [11], while amorphous Al_2O_3 turned polycrystalline at higher than 800°C temperatures [36, 37]. Mixing materials which have different crystallization temperatures might increase the resistance of a new mixture structure to crystallization during annealing [2, 12, 38, 39]. For example, the binary mixtures of HfO_2, Sc_2O_3 and Al_2O_3 might remain amorphous after high temperature annealing, having low scatter losses compared to their pure constituents. Moreover, using such mixtures within multilayer stacks might lead to the increased laser induced damage threshold (LIDT) of optical coatings to ultrashort pulses due to the increased mixture bandgap, as it was shown in the study of Mangote et al. [25]. The investigation of high and medium refractive index material mixture properties might lead to the identification of possible combinations for the design of stress compensated high LIDT multilayer coatings for the UV spectral range.

In this paper, the investigation of optical, surface and stress properties of binary HfO_2, Sc_2O_3 and Al_2O_3 mixtures of different mixing ratios including thermal annealing up to 900°C is presented. Possible applications for designing stress compensated low surface roughness, amorphous multilayer coatings for the UV spectral range are discussed.

2. Methods

Fused silica (FS) substrates (25.4 mm diameter and 1 mm thickness) were cleaned in alkali solution, followed by tap water, then by deionized water and dried in 50°C air before the coating process. Coatings were prepared using an IBS coating plant Navigator 900 (*Cutting Edge Coatings GmbH*) equipped with an Ar^+ ion source and a zone target. Three metal targets of 200 × 200 mm size – Hf, Sc and Al – were used for making relevant oxide layers and corresponding binary mixture layers. The position of the combined binary metal target (400 × 200 mm) centre with respect to the bombarding Ar^+ ion beam determined the final mixture composition. Exposed different material areas were sputtered simultaneously, resulting in a mixture layer. Accelerating voltage of 1200 V was used for the extraction of Ar^+ ions. A neutralizer was used to supply electrons for the suppression of charge build up in the chamber.

O_2 gas was introduced into a vacuum chamber to ensure the oxidation of a growing layer. Different metals needed different optimal oxygen flows for proper oxidation (Hf 7 sccm, Sc 10 sccm, Al 30 sccm). The deposition control software was using linearly interpolated oxygen flow values while making mixture layers, depending on the target position and the used oxygen flow values of pure material. The samples were rotated at 30 rpm and no additional sample heating during the process was used. The typical deposition rates were from 0.6 to 1 Å/s.

The optical thickness of 7 quarter wavelength at 355 nm was chosen for making mixture films. Optical thicknesses of growing films were monitored by comparing the *in situ* measured 400–1000 nm spectrum using an integrated broadband spectrometer with a synthetic spectrum. Since the refractive index was different for each mixture case, this resulted in different physical thicknesses between 290 and 360 nm. The prepared samples were annealed in air at 300, 500, 600, 700, 800 and 900°C using a SNOL 8.2/1100 heating furnace. Target temperatures were achieved using a heating rate of 1°C/min, and then the samples were baked for one hour. Cooling down occurred by turning off the furnace heating. The film thickness, the dispersion of the index of refraction, and the extinction coefficient were determined by fitting the measured transmittance spectrum (Lambda 950, *Perkin Elmer*) with the OptiChar software. Good agreement between the measured and model spectra was observed in all cases. The volumetric fractions of materials in the mixture films were estimated by modelling transmittance spectra in a low absorption spectral zone with OptiChar and using Bruggemann's formula in effective medium theory [40]. Volumetric fractions for HfO_2–Sc_2O_3 mixtures were not calculated because the similarity of refractive indices of those materials resulted in almost identical transmittance spectra even for different mixture cases. The deposition rates of hafnia and scandia were similar, so the zone target position was used for the rough volumetric fraction estimation, as presented in Table 1.

For the sake of simplicity, only the percentage of higher n material within the mixture is further denoted. For example, taking the HfO_2–Sc_2O_3 case, only an approximate hafnia fraction will be indicated. Stoney's formula [41] was applied to calculate the residual stress of films using the uncoated and coated substrate curvature measurement average for two perpendicular directions by a Dektak 150 profilometer (*Veeco*). Tensile stress was considered as a negative and compressive stress as a positive one. Film surface roughness was investigated using a Dimension Edge (*Veeco*) atomic force microscope (AFM) in the tapping mode. Three 20 × 20 μm size areas at different places were scanned and the average calculated values were used for the analysis.

Table 1. Approximate volumetric fractions of HfO_2–Sc_2O_3 mixtures.

Target position, mm	HfO_2 fraction, %	Sc_2O_3 fraction, %
15	100	0
100	70	30
130	50	50
160	30	70
250	0	100

3. Results and analysis

3.1. Surface properties

Ion beam sputtered layers are amorphous, but can change their phase to the polycrystalline one after annealing to higher temperatures [10, 30]. Many studies demonstrated that the surface roughness of a crystalline thin film is considerably higher compared to the amorphous one [42–46]. The evolution of the surface roughness root mean square (RMS) after each annealing step of the samples

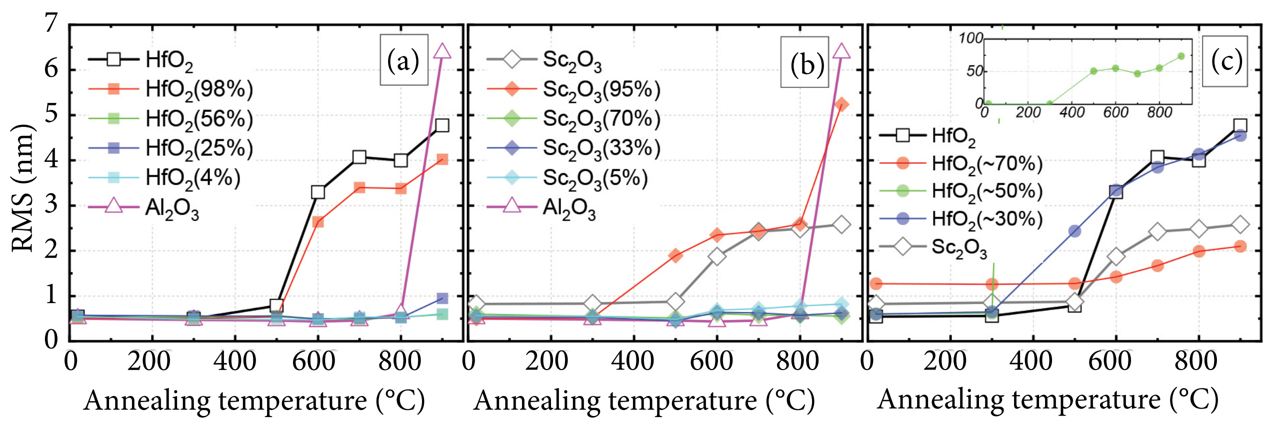

Fig. 1. Surface roughness evolution of HfO_2, Al_2O_3 and Sc_2O_3 and their binary mixture films after thermal annealing at chosen temperatures.

was analyzed. The phase change for HfO_2 and HfO_2 (98%) mixture layers appeared in the 500–600 °C range, though annealing at 500 °C already resulted in a slight RMS increase from initial 0.54 to 0.78 nm (Fig. 1(a)). The surface roughness of Al_2O_3 showed a big increase to 6.4 nm after annealing at 900 °C, while it remained almost unchanged from initial 0.52 to 0.6 nm after the T = 700 °C treatment. A surprising and interesting fact is that admixing just 4% HfO_2 material, which is much more sensitive to annealing-induced crystallization, resulted in the crystallization resistant mixture up to the T = 900 °C treatment (RMS = 0.6 nm) layer (cyan curve in Fig. 1(a)). Other intermediate hafnia–alumina mixtures layers (HfO_2(56%) and HfO_2(25%)) retained the initial surface roughness after T = 800 °C annealing. These results are in line with investigations of hafnium aluminate and its observed crystallization temperature, exceeding 900 °C, though in that work, films were less than 100 nm thick and prepared by pulsed laser deposition [47].

Scandia underwent phase transition in the 500–600 °C range (Fig. 1(b)). Adding 5% of Al_2O_3 to scandia shifted the transition point to even lower temperature (300–500 °C range), while other intermediate Sc_2O_3–Al_2O_3 mixtures (Sc_2O_3(70%) and Sc_2O_3(33%)) did not change their surface roughness even after annealing at 900 °C (0.55 and 0.62 nm, respectively). It is clearly seen that for both cases adding Al_2O_3 in the range from 30 to 75% allows the suppression of crystallization and the extension of possible annealing temperatures up to 900 °C.

The HfO_2(70%)–Sc_2O_3 mixture already had a higher initial roughness of 1.3 nm, which may indicate a polycrystalline structure. Its surface roughness slightly increased with the increase of annealing temperature. Other HfO_2–Sc_2O_3 mixtures demonstrated phase transition temperatures in ranges of 300° ≤ T ≤ 500 °C and 500° ≤ T ≤ 600 °C. Overall, they are much less stable under the influence of medium temperature annealing, compared to other binary mixtures with Al_2O_3.

3.2. Optical properties

The refractive indices of binary mixtures were dependent on volumetric fractions. They increased with the increase of the fraction of higher refractive index material (HfO_2 or Sc_2O_3) within the mixture (Fig. 1(a, b)). Several material mixture-related

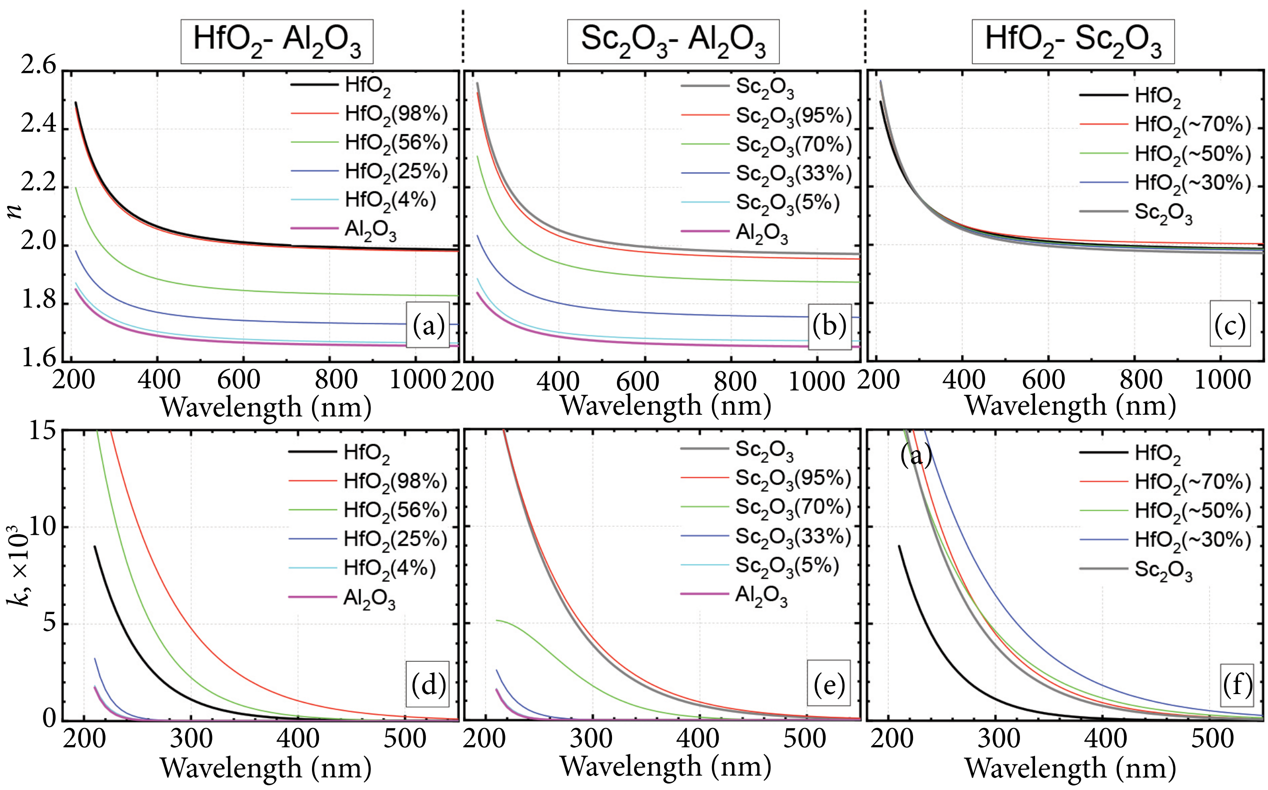

Fig. 2. Refractive index (a, b, c) and extinction coefficient (e, f, g) dispersions of HfO_2, Al_2O_3, Sc_2O_3 and their binary mixture films.

studies also reported similar trends while combining higher and lower refractive index materials [14, 26, 27]. The refractive indices of all hafnia–scandia mixtures were very close, since both pure materials have very similar optical properties. Extinction coefficients of the HfO_2(98%), HfO_2(56%) and mixture layers were higher than for the pure HfO_2 (Fig. 2(d)). Hafnia is very sensitive to backfill oxygen flow during the sputtering process. Also, the optimal amounts of oxygen are different for alumina and scandia. For all mixtures deposition oxygen flow values were calculated using a simple interpolation between the values of respective pure materials and most likely were not optimal. On the other hand, the optimization of mixtures extinction was not the scope of this work. This could be investigated and optimized in future research. Extinction decreased for the Sc_2O_3–Al_2O_3 mixtures with the increased fraction of less absorbing Al_2O_3 material (Fig. 2(e)). As for the HfO_2–Sc_2O_3 mixtures, their extinctions were close to Sc_2O_3, except the HfO_2(~30%)–Sc_2O_3 sample (Fig. 2(f)).

Figure 3(a, b, c) shows the changes in the refractive indices at 355 nm and the wavelength $\lambda_{0.001}$ values after annealing. This wavelength is defined for which material extinction is $k = 0.001$. The decrease of $\lambda_{0.001}$ values means that layer extinction decreases and it becomes more transparent in the UV spectral range. The refractive indices of hafnia and HfO_2(98%) mixture (Fig. 3(a)) constantly decreased under annealing. Intermediate mixtures after a slight 1.5% decrease of refractive indices because of 500 °C annealing more or less did not suffer further changes up to 800 °C, while after the 900 °C treatment, the refractive indices returned to their initial values. The extinction of pure hafnia and its mixtures (98 and 56%) was constantly decreasing while annealing up to 500 °C (Fig. 3(d)). This could be attributed to the increased oxidation and the improved stoichiometry of deposited layers [33, 48, 49]. Annealing further at 600 °C increased the extinction of HfO_2 and HfO_2 (98%), which most likely is the result of increased optical scatter after crystallization that is accompanied by strongly increased layers surface RMS (Fig. 1(a)). All other hafnia–alumina mixtures demonstrated a smaller, slightly decreasing or constant extinction throughout the all

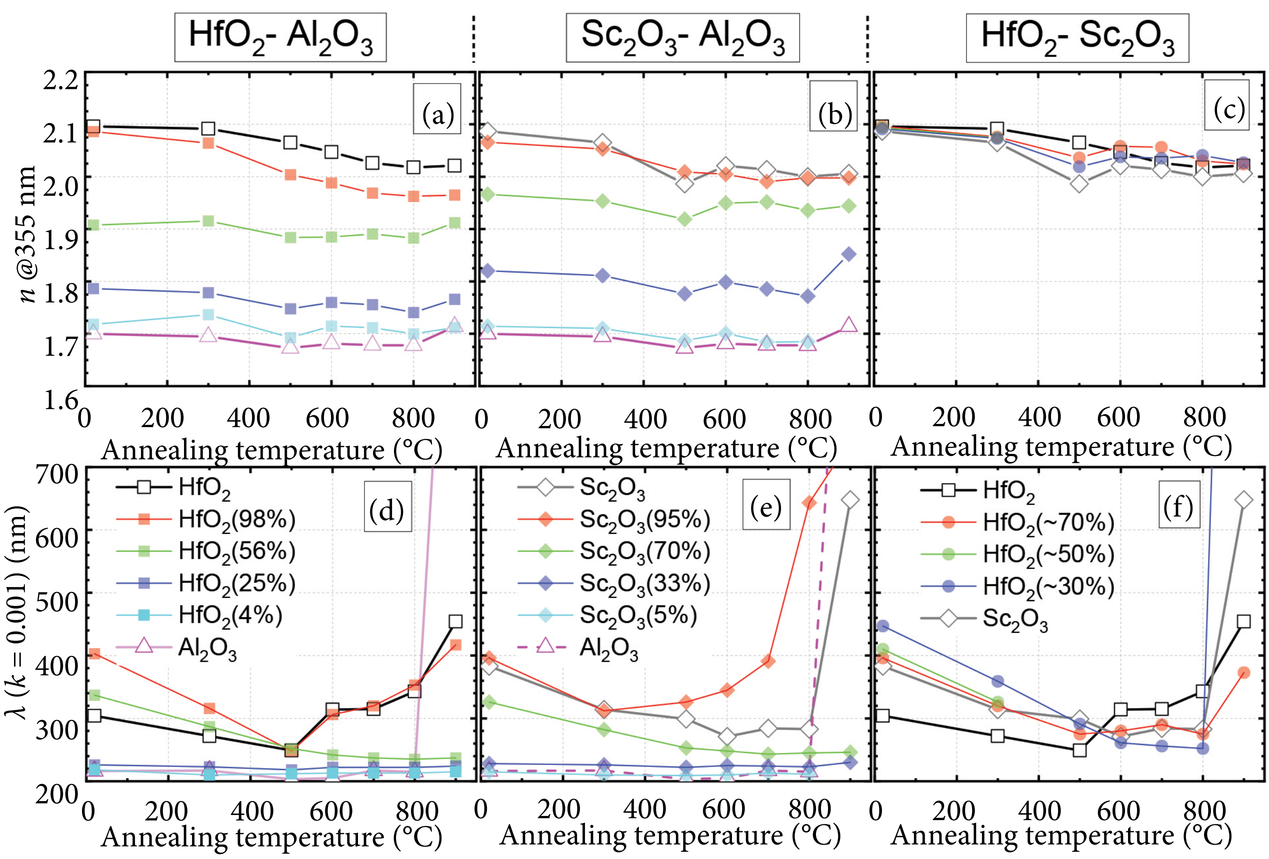

Fig. 3. Refractive index and λ ($k = 0.001$) after the thermal annealing of HfO_2–Al_2O_3 (a, d), Sc_2O_3–Al_2O_3 (b, e) and HfO_2–Sc_2O_3 (c, f) mixture films. Legends in bottom graphs are similar for the corresponding top graphs.

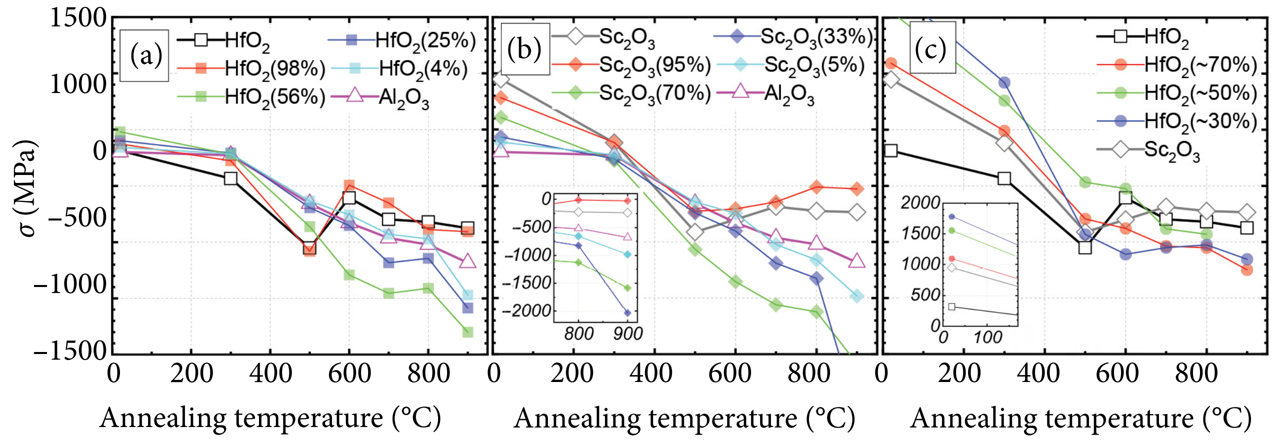

Fig. 4. HfO_2–Al_2O_3 (a), Sc_2O_3–Al_2O_3 (b) and HfO_2–Sc_2O_3 (c) mixture film stress evolution with the increase of annealing temperature.

annealing range. Pure Al_2O_3 suffered a drastically increased extinction after annealing in 900 °C, due to the phase change to a crystalline structure, as it was also reported in several works [36, 37].

The refractive index n of Sc_2O_3 decreased after initial annealing. After the crystallization at $500° \le T \le 600$ °C, it increased and then a slight decrease was further observed. n of other Sc_2O_3–Al_2O_3 mixtures followed the same trend as scandia, except the mixture with 5% of alumina, the refractive index of which had a constantly decreasing trend. The extinction k of Sc_2O_3 decreased after each annealing step, even after the crystallization. That might mean that small crystallites were present within the polycrystalline material and did not contribute to optical loss, which dramatically rose after annealing at 900 °C. However, the observed phenomenon needs additional material structural analysis. The Sc_2O_3(95%) mixture underwent phase change after treating at 500 °C, and the extinction constantly increased while annealing at higher temperatures. The intermediate mixtures (70, 33, 5%) demonstrated a constantly decreasing or unchanged extinction.

The refractive indices of HfO_2–Sc_2O_3 mixtures followed intermediate trends between their pure counterpart materials until 500 °C annealing. However, using 700 °C annealing, n of HfO_2(~70%)–Sc_2O_3 slightly exceeded (by 1.5%) the value of HfO_2. The extinction of composite films was bigger than those of hafnia or scandia. After annealing to 600 °C, the extinction of HfO_2(~30%)–Sc_2O_3 became the smallest one of all samples. The HfO_2(~50%)–Sc_2O_3 mixture suffered phase change and an extremely increased surface roughness up to 50 nm (Fig. 1(c)) after the 500 °C treatment, leading to high optical losses. Due to this, there are no extinction data points presented for this mixture above 300 °C. Annealing at 900 °C increased k for all samples, and this could not be related just due to scatter losses, because roughness remained almost unchanged or even reduced for the HfO_2(~70%)–Sc_2O_3 case (Fig. 1(c)).

3.3. *Stress properties*

The residual stresses of deposited and post-annealed samples are presented in Fig. 4. The pure hafnia and hafnia mixture with the 2% alumina content demonstrated a rapid decrease of initial stress by $\Delta\sigma = 860$ MPa, after annealing at 500°C reaching tensile stresses of ~ −560 MPa (Fig. 4(a)). The most interesting behaviour was observed for the as-deposited HfO_2(56%) and HfO_2(25%) mixture films. Their initial stresses were bigger by $\Delta\sigma = 170$ MPa and $\Delta\sigma = 90$ MPa, respectively, than those of HfO_2 or Al_2O_3. The stresses turned to tensile after annealing at 500°C. Even more, after next two baking steps (600 and 700°C), the tensile stresses further increased, especially for the HfO_2(56%) mixture. Peculiar changes in the stress amplitude are clearly seen after annealing at 900°C, with HfO_2(56%) reaching −1300 MPa and HfO_2(25%) reaching −1090 MPa. It is important to note that these two mixtures after the treatments in the 700–900 °C range act differently and possess bigger tensile stresses than their constituents – HfO_2 and Al_2O_3.

The stress values of deposited Sc_2O_3–Al_2O_3 mixtures (Fig. 4(b)) were distributed between the stress values of pure materials. After annealing at 500°C, the stresses of scandia and Sc_2O_3(95%) mixture films became tensile. However, after baking at 600°C, the values shifted back towards zero. This could be attributed to the stress relief due to coating cracking, which was observed by an optical microscope. Other mixtures also demonstrated change from compressive to tensile stresses after T_c = 500 °C, which increased further after the higher temperature treatment. The highest $\Delta\sigma$ was observed for the Sc_2O_3(70%) mixture which reached −1580 MPa after the 900 °C treatment.

All deposited HfO_2–Sc_2O_3 mixtures show higher compressive stresses than constituent materials. They were reduced after initial annealing stages, but after treating to T > 600°C, further changes in tensile stress values remained small.

The changes of ion beam sputtered SiO_2 film stress after annealing are presented in the Kičas et al. work [8]. Annealed SiO_2 layers obtain the following compressive stresses: ~380 MPa (400°C) and ~225 MPa (500°C). Low-n SiO_2 layers are thicker than high-n layers in the standard Bragg dielectric mirror stack. The actual difference in physical thicknesses depends on the refractive index contrast between the stack materials. In order to obtain the total coating stress close to zero by thermal treatment, high-n material should have a higher tensile stress than SiO_2 compressive stress. For more complex multilayer coatings, like filters, polarizers, and narrow reflectance band mirrors, the total thickness of SiO_2 layers might be even much greater than those of the high refractive index material layers. In such case, higher annealing temperatures might be necessary or higher tensile stress of other stack material should be achieved. The following high-n binary mixtures are presented in Table 2 as potential candidates for designing of stress-compensated multilayer IBS coatings for the UV spectral range. It should also be noted that using a hafnia–alumina or scandia–alumina mixture in multilayer coating would also result in higher resistance to high power laser pulses due to a higher bandgap of mixture material compared with pure hafnia or scandia, as was demonstrated in other research [50]. The hafnia–scandia mixture stands out with the highest refractive index of all listed candidates but it also has slightly higher extinction values and a considerably higher film surface roughness. In general, all these selected binary mixes (Table 2) should be treated as a starting point for further tuning and optimization experiments changing mixture ratios and process parameters like oxygen flow in order to decrease extinction and surface roughness (for the hafnia–scandia mixture case). It is also important to understand that precise annealing temperatures for obtaining the zero net stress of the multilayer stack with SiO_2 would be dependent on the ratio of the chosen mixture material and SiO_2 thickness. They should lie in the range of 400° ≤ T ≤ 600°C.

4. Conclusions

Binary HfO_2, Sc_2O_3 and Al_2O_3 mixtures of different ratios were prepared by the IBS coating process. Optical, surface and stress properties using thermal post deposition annealing up to 900°C were analyzed. HfO_2–Al_2O_3 mixtures demonstrated higher extinction than their pure components, so its minimization is the task for the future process optimization. Annealing helped to decrease the extinction of the most mixture layers with the higher content of HfO_2 or Sc_2O_3, while further changes using higher than 600°C treatments were not significant. The refractive indices of mentioned mixtures remained more or less unchanged, while the pure HfO_2 and Sc_2O_3 layers demonstrated a constant decrease of the refractive index with the increase of annealing temperatures.

Table 2. Potential binary mixtures for designing stress compensated coatings for the UV spectral range.

Binary mixture	Annealing temperature range, °C	Stress, MPa	n, 355 nm	Surface roughness RMS, nm
HfO_2(56%)–Al_2O_3(44%)	500–600	−360…−790	1.884	0.57
Sc_2O_3(70%)–Al_2O_3(30%)	500–600	−560…−850	1.919–1.95	0.51–0.61
HfO_2(~70%)–Sc_2O_3(~30%)	500–600	−295…−380	2.036–2.058	1.28–1.42

Admixing Al_2O_3 to HfO_2 and Sc_2O_3 also allowed one to keep an initial low surface roughness after annealing even to 800–900°C temperatures which suggest a remaining amorphous structure of the layers.

Several high-*n* binary mixtures – HfO_2(56%)–Al_2O_3(44%), Sc_2O_3(70%)–Al_2O_3(30%) and HfO_2 (~70%)–Sc_2O_3(~30%) – were identified which did not show the increase of surface roughness and extinction in the UV spectral range even after annealing at temperatures as high as 800–900°C. Moreover, these mixtures respectively possess tensile stress values of –360, –560 and –295 MPa if using 500°C annealing. Compressive stresses of low refractive index SiO_2 layers within the multilayer stack could be compensated by mixture layers by choosing annealing temperature in a range of $400° \leq T \leq 600°$C depending on the physical thickness ratio between both materials within the coating stack. For real cases, additional experiments would be needed to determine required optimal annealing temperatures. The obtained results show good perspectives designing and obtaining stress balanced and potentially enhanced LIDT multilayer IBS coatings for the UV spectral range, employing selected HfO_2–Al_2O_3, Sc_2O_3–Al_2O_3 and HfO_2–Sc_2O_3 mixtures as high refractive index materials and post-deposition thermal annealing at optimized temperatures.

Acknowledgements

I would like to express my appreciation and gratitude to Tomas Juodagalvis for assisting in the experimental work.

References

[1] N. Demos, S. Gras, M. Evans, P. O'Brien, G. Billingsley, and L. Zhang, Substoichiometric silica in a multimaterial highly reflective coating, Class. Quant. Grav. **42**, 115012 (2025).

[2] A. Amato, G. Cagnoli, M. Granata, B. Sassolas, J. Degallaix, D. Forest, C. Michel, L. Pinard, N. Demos, and S. Gras, Optical and mechanical properties of ion-beam-sputtered Nb_2O_5 and TiO_2-Nb_2O_5 thin films for gravitational-wave interferometers and an improved measurement of coating thermal noise in Advanced LIGO, Phys. Rev. D **103**, 072001 (2021).

[3] G.-W. Truong, L.W. Perner, D.M. Bailey, G. Winkler, S.B. Cataño-Lopez, V.J. Wittwer, T. Südmeyer, C. Nguyen, D. Follman, and A.J. Fleisher, Mid-infrared supermirrors with finesse exceeding 400 000, Nat. Commun. **14**, 7846 (2023).

[4] C.-J. Tang, C.-C. Jaing, K.-S. Lee, and C.-C. Lee, Residual stress in Ta_2O_5-SiO_2 composite thin-film rugate filters prepared by radio frequency ion-beam sputtering, Appl. Opt. **47**, C167 (2008).

[5] R. Thielsch, A. Gatto, and N. Kaiser, Mechanical stress and thermal-elastic properties of oxide coatings for use in the deep-ultraviolet spectral region, Appl. Opt. **41**, 3211 (2002).

[6] O. Stenzel, M. Schürmann, S. Wilbrandt, N. Kaiser, A. Tünnermann, M. Mende, H. Ehlers, D. Ristau, S. Bruns, M. Vergöhl, et al., Optical and mechanical properties of oxide UV coatings, prepared by PVD techniques, SPIE OSD **8168**, 10 (2011).

[7] C. Malhaire, M. Granata, D. Hofman, A. Amato, V. Martinez, G. Cagnoli, A. Lemaitre, and N. Shcheblanov, Determination of compressive stress in thin films using micro-machined buckled membranes, arXiv:2305.15794 (2023).

[8] S. Kičas, U. Gimževskis, and S. Melnikas, Post deposition annealing of IBS mixture coatings for compensation of film induced stress, Opt. Mater. Express **6**, 2236 (2016).

[9] D.J. Reiley and R.A. Chipman, Coating-induced wave-front aberrations: on-axis astigmatism and chromatic aberration in all-reflecting systems, Appl. Opt. **33**, 2002 (1994).

[10] M. Bischoff, T. Nowitzki, O. Voß, S. Wilbrandt, and O. Stenzel, Postdeposition treatment of IBS coatings for UV applications with optimized thin-film stress properties, Appl. Opt. **53**, A212 (2014).

[11] M. Falmbigl, K. Godin, J. George, C. Mühlig, and B. Rubin, Effect of annealing on properties and performance of HfO_2/SiO_2 optical coatings for UV-applications, Opt. Express **30**, 12326 (2022).

[12] C. Harthcock, H.T. Nguyen, D. Vipin, and M. Huang, Impact of high-temperature annealing on hafnia-silica composite coatings deposited via ion beam sputtering for high-peak power 1064 nm lasers, Opt. Mater. Express **15**, 2592 (2025).

[13] W.-H. Wang and S. Chao, Annealing effect on ion-beam-sputtered titanium dioxide film, Opt. Lett. **23**, 1417 (1998).

[14] S. Chao, W.-H. Wang, M.-Y. Hsu, and L.-C. Wang, Characteristics of ion-beam-sputtered high-refractive-index TiO_2-SiO_2 mixed films, J. Opt. Soc. Am. A **16**, 1477 (1999).

[15] G. Favaro, V. Milotti, D. Alonso Diaz Riega, N. Busdon, M. Bazzan, M. Granata, D. Hofman, C. Michel, L. Pinard, L. Conti, et al., Reduction of mechanical losses in ion-beam sputtered tantalum oxide thin films via partial crystallization, Class. Quant. Grav. **41**, 105009 (2024).

[16] M. Steinecke, K. Kiedrowski, M. Jupé, and D. Ristau, Very thick mixture oxide ion beam sputtering films for investigation of nonlinear material properties, Eur. Phys. J. Appl. Phys. **80**, 30301 (2017).

[17] E. Randel, A. Davenport, A. Markosyan, R. Bassiri, M.M. Fejer, and C.S. Menoni, Ultra-low stress SiO_2 ion beam deposition coatings, in: *Proceedings of the Optical Interference Coatings Conference (OIC) 2019*, Optical Society of America (2019) pp. WC.5.

[18] E. Çetinörgü, B. Baloukas, O. Zabeida, J.E. Klemberg-Sapieha, and L. Martinu, Mechanical and thermoelastic characteristics of optical thin films deposited by dual ion beam sputtering, Appl. Opt. **48**, 4536 (2009).

[19] P.F. Langston, E. Krous, D. Schiltz, D. Patel, L. Emmert, A. Markosyan, B. Reagan, K. Wernsing, Y. Xu, Z. Sun, et al., Point defects in Sc_2O_3 thin films by ion beam sputtering, Appl. Opt. **53**, A276 (2014).

[20] H. Liu, Y. Jiang, L. Wang, J. Leng, P. Sun, K. Zhuang, Y. Ji, X. Cheng, H. Jiao, Z. Wang, and B. Wu, Correlation between properties of HfO_2 films and preparing parameters by ion beam sputtering deposition, Appl. Opt. **53**, A405 (2014).

[21] Z. Qiao, Y. Pu, H. Liu, K. Luo, G. Wang, Z. Liu, and P. Ma, Residual stress and laser-induced damage of ion-beam sputtered Ta_2O_5/SiO_2 mixture coatings, Thin Solid Films **592**, 221 (2015).

[22] B.J. Pond, J.I. DeBar, C.K. Carniglia, and T. Raj, Stress reduction in ion beam sputtered mixed oxide films, Appl. Opt. **28**, 2800 (1989).

[23] S. Melnikas, U. Gimževskis, and S. Kičas, Stress compensated back side coated chirped mirror with high negative dispersion, Opt. Laser Technol. **121**, 105820 (2020).

[24] L. O. Jensen, M. Mende, H. Blaschke, D. Ristau, D. Nguyen, L. Emmert, and W. Rudolph, Investigations on SiO_2/HfO_2 mixtures for nanosecond and femtosecond pulses, Proc. SPIE **7842**, 10 (2010).

[25] B. Mangote, L. Gallais, M. Commandré, M. Mende, L. Jensen, H. Ehlers, M. Jupé, D. Ristau, A. Melninkaitis, J. Mirauskas, et al., Femtosecond laser damage resistance of oxide and mixture oxide optical coatings, Opt. Lett. **37**, 1478 (2012).

[26] X. Fu, M. Commandré, L. Gallais, M. Mende, H. Ehlers, and D. Ristau, Laser-induced damage in composites of scandium, hafnium, aluminum oxides with silicon oxide in the infrared, Appl. Opt. **53**, A392 (2014).

[27] M. Mende, I. Balasa, H. Ehlers, D. Ristau, D.-be Douti, L. Gallais, and M. Commandré, Relation of optical properties and femtosecond laser damage resistance for Al_2O_3/AlF_3 and Al_2O_3/SiO_2 composite coatings, Appl. Opt. **53**, A383 (2014).

[28] L.O. Jensen, and D. Ristau, Coatings of oxide composites, Proc. SPIE **8530**, 15 (2012).

[29] H. Blaschke, M. Lappschies, and D. Ristau, Performance enhancement of ion beam sputtered oxide coatings for 193 nm, SPIE **6720**, 10 (2007).

[30] G. Abromavičius, S. Kičas, and R. Buzelis, High temperature annealing effects on spectral, microstructural and laser damage resistance properties of sputtered HfO_2 and HfO_2-SiO_2 mixture-based UV mirrors, Opt. Mater. **95**, 109245 (2019).

[31] H. Grüger, C. Kunath, E. Kurth, S. Sorge, W. Pufe, and T. Pechstein, High quality r.f. sputtered metal oxides (Ta_2O_5, HfO_2) and their properties after annealing, Thin Solid Films **447–448**, 509 (2004).

[32] C.-C. Lee, C.-L. Tien, W.-S. Sheu, and C.-C. Jaing, An apparatus for the measurement of internal stress and thermal expansion coefficient of metal oxide films, Rev. Sci. Instrum. **72**, 2128 (2001).

[33] H. Liu, Y. Jiang, L. Wang, S. Li, X. Yang, C. Jiang, D. Liu, Y. Ji, F. Zhang, and D. Chen, Effect of heat treatment on properties of HfO_2 film deposited by ion-beam sputtering, Opt. Mater. **73**, 95 (2017).

[34] G. He, M. Liu, L.Q. Zhu, M. Chang, Q. Fang, and L.D. Zhang, Effect of postdeposition annealing on the thermal stability and structural characteristics of sputtered HfO_2 films on Si (100), Surf. Sci. **576**, 67 (2005).

[35] J.-W. Park, D.-K. Lee, D. Lim, H. Lee, and S.-H. Choi, Optical properties of thermally annealed hafnium oxide and their correlation with structural change, J. Appl. Phys. **104**, 033521 (2008).

[36] V. Edlmayr, M. Moser, C. Walter, and C. Mitterer, Thermal stability of sputtered Al_2O_3 coatings, Surf. Coat. Technol. **204**, 1576 (2010).

[37] S. Jakschik, U. Schroeder, T. Hecht, M. Gutsche, H. Seidl, and J.W. Bartha, Crystallization behavior of thin ALD-Al_2O_3 films, Thin Solid Films **425**, 216 (2003).

[38] V. Milotti, G. Favaro, M. Granata, D. Forest, C. Michel, J. Teillon, N. Busdon, M. Bazzan, H. Skliarova, and G. Ciani, Thermal noise reduction in ion-beam sputtered HfO_2: Ta_2O_5 thin films via high-temperature treatment, Opt. Mater. **163**, 116901 (2025).

[39] Z.L. Pei, L. Pereira, G. Gonçalves, P. Barquinha, N. Franco, E. Alves, A.M.B. Rego, R. Martins, and E. Fortunato, Room-temperature cosputtered HfO_2-Al_2O_3 multicomponent gate dielectrics, Electrochem. Solid-State Lett. **12**, G65 (2009).

[40] T. Tolenis, M. Gaspariūnas, M. Lelis, A. Plukis, R. Buzelis, and A. Melninkaitis, Assessment of effective-medium theories of ion-beam sputtered Nb_2O_5–SiO_2 and ZrO_2–SiO_2 mixtures, Lith. J. Phys. **54** (2014).

[41] G.G. Stoney, The tension of metallic films deposited by electrolysis, Proc. R. Soc. Lond. A **82**, 172 (1909).

[42] J. Wang, R.L. Maier, and H. Schreiber, Crystal phase transition of HfO_2 films evaporated by plasma-ion-assisted deposition, Appl. Opt. **47**, C189 (2008).

[43] C.J. Stolz, F.Y. Genin, M.R. Kozlowski, D. Long, R. Lalazari, Z. Wu, and P.-K. Kuo, Influence of microstructure on laser damage threshold of IBS coatings, Proc. SPIE **2714**, 9 (1996).

[44] J. Gao, G. He, B. Deng, D.Q. Xiao, M. Liu, P. Jin, C.Y. Zheng, and Z.Q. Sun, Microstructure, wettability, optical and electrical properties of HfO_2 thin films: Effect of oxygen partial pressure, J. Alloys Compd. **662**, 339 (2016).

[45] C. Xu, Y. Qiang, Y. Zhu, T. Zhai, L. Guo, Y. Zhao, J. Shao, and Z. Fan, Laser-induced damage threshold at different wavelengths of Ta_2O_5 films annealed over a wide temperature range, Vacuum **84**, 1310 (2010).

[46] Z. Balogh-Michels, I. Stevanovic, A. Borzi, A. Bächli, D. Schachtler, T. Gischkat, A. Neels, A. Stuck, and R. Botha, Crystallization behavior of ion beam sputtered HfO_2 thin films and its effect on the laser-induced damage threshold, J. Eur. Opt. Soc. Rapid Publ. **17**, 3 (2021).

[47] X.Y. Qiu, Q.M. Liu, F. Gao, L.Y. Lu, and J.-M. Liu, Room-temperature weak ferromagnetism of amorphous $HfAlO_x$ thin films deposited by pulsed laser deposition, Appl. Phys. Lett. **89**, 242504 (2006).

[48] C. Xu, H. Dong, L. Yuan, H. He, J. Shao, and Z. Fan, Investigation of annealing effects on the laser-induced damage threshold of amorphous Ta_2O_5 films, Opt. Laser Technol. **41**, 258 (2009).

[49] Y. Zhao, Y. Wang, H. Gong, J. Shao, and Z. Fan, Annealing effects on structure and laser-induced damage threshold of Ta_2O_5/SiO_2 dielectric mirrors, Appl. Surf. Sci. **210**, 353 (2003).

[50] J. Shi, M. Zhu, W. Du, T. Liu, L. Zhou, Y. Jiang, J. Sun, J. Li, and J. Shao, Picosecond laser-induced damage of HfO_2-Al_2O_3 mixture-based mirror coatings in atmosphere and vacuum environments, Opt. Mater. Express **13**, 667 (2023).

JONAPLUOŠČIO DULKINIMO BŪDU SUFORMUOTŲ IR ATKAITINTŲ IKI AUKŠTŲ TEMPERATŪRŲ HfO_2, Sc_2O_3 IR Al_2O_3 MIŠINIŲ SLUOKSNIŲ ĮTEMPIŲ, OPTINIŲ IR PAVIRŠINIŲ SAVYBIŲ TYRIMAS

G. Abromavičius

Fizinių ir technologijos mokslų centro Optinių dangų laboratorija, Vilnius, Lietuva

Santrauka

Dideli vidiniai įtempiai yra vienas didžiausių jonapluoščio dulkinimo būdu suformuotų optinių dangų trūkumų, mažinančių optinių komponentų plokštiškumą. Aukšto lūžio rodiklio metalų oksidų mišiniai su SiO_2 leidžia padidinti daugiasluoksnių dangų lazerio indukuotos pažaidos slenkstį. Tyrime pateikiama HfO_2-Al_2O_3, Sc_2O_3-Al_2O_3, HfO_2-Sc_2O_3 mišinių sluoksnių įtempių, optinių ir paviršinių savybių analizė, taikant terminį atkaitinimą plačiame temperatūrų ruože – nuo 300 iki 900 °C. Suformavus HfO_2 ir Sc_2O_3 sluoksnius, pasižyminčius vidutinio dydžio Al_2O_3 frakcijomis, galima išlaikyti žemą pradinį sluoksnių paviršiaus šiurkštumą, mažėjančią ekstinkciją, taikant terminį atkaitinimą iki aukštų temperatūrų. Šie mišiniai taip pat pasižymi −360...−560 MPa tempiamaisiais įtempiais po kaitinimo iki 500 °C. Gauti duomenys leidžia identifikuoti perspektyvius HfO_2(56 %)-Al_2O_3(44 %), Sc_2O_3(70 %)-Al_2O_3(30 %), HfO_2(~70 %)-Sc_2O_3(~30 %) mišinius ir 500–600 °C atkaitinimo temperatūrų ruožą, tinkamus daugiasluoksnių UV optinių dangų projektavimui su kompensuotais įtempiais bei potencialiai didesniu lazerinės pažaidos slenksčiu.